Bull. Inst. Chem. Res., Kyoto Univ., Vol.72, No.1, 1994

Quasi-free Process in the ^{6}Li(α,^{3}He^{5}He)^{2}H Reaction at E_{α} = 119 MeV

Tadahiko YOSHIMURA, Akira OKIHANA, Shigeru KAKIGI*, R. E. WARNER**, Mamoru FUJIWARA***, Nobuyuki MATSUOKA***, Kiyoji FUKUNAGA†, Toshiharu HAYASHI*, Jirota KASAGI††, Mituo TOSAKI‡ and M. B. GREENFIELD‡‡

Received February 10, 1994

Cross sections for the ^{6}Li (α, α ^{3}He) reaction were measured at E_{inc} = 119 MeV in coplanar geometry. In continuum energy regions of the energy maps, some enhancements which correspond to QF peaks of the $\alpha + \alpha \rightarrow {}^{3}\mathrm{He} + {}^{5}\mathrm{He}$ QFR in the ^{6}Li (α,^{3}He^{5}He)^{2}H reaction, were seen. At zero recoil momentum, three-body breakup cross sections for the ^{6}Li (α,^{3}He^{5}He)^{2}H reaction were deduced from the measured cross sections for the ^{6}Li (α, α ^{3}He) reaction by considering detection efficiencies of ^{5}He. The detection efficiencies were estimated using the Monte Carlo method. In the analysis of the reaction, the PWIA was applied, by which two-body cross sections of the elementary process in this QFR were deduced from the three-body cross sections. The deduced two-body cross sections were normalized to a free cross section for the ^{4}He (α,^{3}He)^{5}He reaction and compared with the angular distribution of the free cross sections. The deduced two-body cross sections were almost agree with the angular distribution.

KEY WORDS: Nuclear reaction ^{6}Li (α,^{3}He^{5}He)^{2}H / E = 119 MeV / Quasi-free Reaction / Plane Wave Impluse Approximation / Detection Efficiency of ^{5}He

1. INTRODUCTION

Quasi-free knockout reactions such as (p,pα), (α,2α) and (e,e'α) have been studied to investigate α cluster structures in nuclei or reaction mechanisms. In the analyses of these reactions, mainly, the distorted wave impulse approximation (DWIA) or the plane wave impulse approximation (PWIA) have been applied, by extracting the α-spectroscopic factor or the momentum distribution in the nucleus. Since distortion effects in the initial and the final states are important even at intermediate energies, the DWIA prediction is generally more accurate than the PWIA one. Validity of the DWIA in the analysis of the reactions has been examined in many experiments. Especially for the (p,pα) reaction it was positively investigated by Roos et al.[1] and Nadasen et al.[2], who showed that the DWIA calculations reproduce

吉村忠彦、沖花　彰 : Kyoto University of Education, Kyoto 612, Japan
* 柿木　茂、林　俊治 : Institute for Chemical Research, Kyoto University, Kyoto 611, Japan
** R. E. Warner : Oberlin College, Oberlin, OH 44074, USA
*** 藤原　守、松岡伸行 : Research Center for Nuclear Physics, Osaka University, Osaka 567, Japan
† 福永清二 : Yamagata University, Yamagata 990, Japan
†† 笠木治郎太 : Laboratory of Nuclear Science, Tohoku University, Sendai 982, Japan
‡ 戸崎充男 : Radioisotope Research Center, Kyoto University, Kyoto 606, Japan
‡‡ M. B. Greenfield : International Christian University, Tokyo 181, Japan

shapes of the quasi-free peaks in the energy spectra well and the extracted α-spectroscopic factors are good agreement with theoretical predictions, for light nuclei such as ^{6}Li, ^{7}Li, ^{9}Be and ^{12}C at incident energies of 100-200 MeV. On the other hand, for the $(\alpha,2\alpha)$ reaction, in which the distortion effects may be larger than the $(p,p\alpha)$ reaction, validity of the DWIA was shown on ^{9}Be, ^{12}C, ^{16}O and ^{20}Ne at 140 MeV by Wang et al.[3] Also for the $(\alpha,2\alpha)$ reaction on ^{6}Li, it was shown in our works[4] that even at energy of 100 MeV, shapes of the quasi-free peaks are well reproduced by the DWIA calculation and the extracted α-spectroscopic factor is consistent with values of both the $(p,p\alpha)$ reaction and the theory.

These knockout reactions are dominated by the quasi-free scattering (QFS) process which a projectile is directly scattered from a cluster in nucleus, remaining a residual nucleus as a spectator. While there are also knockout reactions which are dominated by other quasi-free (QF) process which is called the quasi-free reaction (QFR) process, in which a projectile (or a cluster) picks up a nucleon or a few nucleons from a cluster (or projectile), remaining a residual nucleus as a spectator. In general, the QFR is more complicate than the QFS because it contains a rearrangement mechanism in the elementary two-body process. So the QFR can not be treated as a simple three-body reaction. Therefore in the QFR, the spectator effect or more than three-body structure in the nucleus may be seen. The QFR has been also studied experimentally and theoretically, but there are not so much studies of the QFR as those of the QFS. In most of them, pickup or stripping processes on "soft" clusters such as deuteron and ^{3}He have been studied[5-9]. Most of these experimental results were analyzed and well reproduced using the PWIA calculation. So it seems that the QFR process with a soft cluster occurs as quasi-freely as the QFS process does. Then, how about the QFR with a hard cluster such as ^{4}He? Cowley et al.[10] studied the $p + \alpha \rightarrow d + {}^{3}He$ QFR in ^{6}Li, ^{7}Li, ^{9}Be and ^{12}C. In the analyses of these reactions, the DWIA calculation reproduced the shapes of the QF peaks and the angular distribution of the elementary process. However, the fitness of the shape of the QF peak by the DWIA seems to be not so good as the case of the QFS. In addition, the agreement of the angular distribution for the elementary process deduced by the DWIA with that for the free process is not sufficient due to the lack of the appropriate free cross section data. Therefore there is yet question about the QFR with a hard cluster and it is worthwhile to examine them comparing with the QFS process.

In this paper, we present an experimental result and a preliminary analysis using the PWIA about the $\alpha + \alpha \rightarrow {}^{3}He + {}^{5}He$ QFR in the ^{6}Li $(\alpha,{}^{3}He{}^{5}He)^{2}$H reaction. The reasons that we choose this reaction, are as follows:

(i). The α-d cluster structure in ^{6}Li has been already well known by studies of the $(p,p\alpha)$ and $(\alpha,2\alpha)$ reactions.

(ii). The result can be compared with the $p + \alpha \rightarrow d + {}^{3}He$ QFR in ^{6}Li, and the QFS process in the ^{6}Li $(\alpha,2\alpha)^{2}$H reaction.

(iii). The angular distribution of the cross sections for the ^{4}He $(\alpha,{}^{3}He)^{5}$He reaction at 120 MeV[11] has been measured accurately, which is the elementary process of the QFR.

2. EXPERIMENTAL PROCEDURE

The experiment was performed using α beam accelerated by the AVF cyclotron at the

Research Center for Nuclear Physics (RCNP) of Osaka University. The bombarding energy at the target center was 119.0 MeV and the beam current was kept between 15 and 20 nA to limit the random coincidence rate. The ^{6}Li target was isotopically enriched to 95.45% and its thickness was 4.0 mg/cm^{2}. Coincident pairs of ^{3}He and α emitted from ^{5}He, were detected by two E-ΔE counter telescopes because ^{5}He can't be detected directly due to its being unbound. The detection efficiencies of ^{5}He were estimated using the Monte Carlo method, which is described in section 4. The telescopes were consisted of a 150 μm ΔE Si-SSD and a 5 mm E Si(Li)-SSD, and were placed on opposite sides of and coplanar with, the beam. The solid angles of the telescopes defined by the slits were about 1.7 msr. The E, ΔE and time signals were transmitted through a raw data processor to a PDP 11/44 computer. The off line analyses were done with the FACOM M1800 computer at RCNP and FACOM M360R computer at Kyoto University of Education. Energy calibration of the telescopes was given both by measuring α + d and α + ^{6}Li elastic scattering and by fitting the three body kinematic loci of the ^{6}Li (α,2α)^{2}H reaction. Particle identification and random-event subtraction were obtained from 2K by 2K, two-dimensional E-ΔE and E-time spectra, respectively. The separations between ^{3}He and ^{4}He as well as between the total and random events were adequate. The measured angle pairs were (θ_{α}, θ_{τ}) = (30.0°, 37.2°), (31.5°, 45.0°), (34.8°, 38.0°), (37.2°, 30.0°), (38.0°, 34.8°) and (45.0°, 31.5°), which correspond to $\theta_{c.m.}$ =74.5°, 90.1°, 76.1°, 60.2°, 69.8° and 63.2°, respectively. $\theta_{c.m.}$ presents an angle in the center of total mass system (CMS) for the elementary process. Only the angle pairs of (37.2°, 30.0°), (34.8°, 38.0°) and (31.5°, 45.0°) satisfy the kinematical condition that the spectator d is rest.

3. EXPERIMENTAL RESULTS

Since this QFR is four-body breakup reaction because ^{5}He decays into an α particle and a neutron, the QF peak is expected to appear in the continuum energy region. The obtained two-dimensional energy spectra are shown in fig. 1. Some enhancements which would correspond to QF peaks were seen in the continuum regions of these spectra as expected. To make sure that these enhancements are yielded from $\alpha + \alpha \rightarrow {}^{3}\mathrm{He} + {}^{5}\mathrm{He}$ QFR, these data were reduced in three ways. Fig. 2 shows one of the spectra removed yields of the ^{6}Li (α, α ^{3}He)^{3}H three-body breakup reaction from them. In the figure, the solid curve presents a kinematical locus of the α^{*}(α, α ^{3}He)n reaction, which corresponds to the elementary process of $\alpha + \alpha \rightarrow {}^{3}\mathrm{He} + {}^{5}\mathrm{He}$ in case of the spectator being rest. α^{*} denotes an α cluster in ^{6}Li. Two crosses on the locus indicate the points where the α + n relative energy is 0.9 MeV, which corresponds to the energy of the g'nd state of ^{5}He. It is seen that the enhancement occurs on these points. Fig. 3 shows the projected spectrum of this map on the E_{τ} axis, where an arrow shows the ^{3}He energy point where the spectator can be rest and the α-n relative energy can be 0.9 MeV. In the figure the peak point of the large bump corresponds to this arrow point. Yields on the locus in the fig. 2 are plotted versus the α-n relative energy, and shown as fig. 4. Shape of the obtained spectrum has two bumps. Each bump has a peak near 1 MeV, which is essentially similar to the spectra of ^{5}He g'nd state which were obtained in our recent experiment[11]. Fig. 2-4 support further that these enhancements are yielded from the $\alpha + \alpha \rightarrow {}^{3}\mathrm{He} + {}^{5}\mathrm{He}$ QFR. This makes sure that the $\alpha + \alpha \rightarrow {}^{3}\mathrm{He} + {}^{5}\mathrm{He}$ QFR process occurs in the

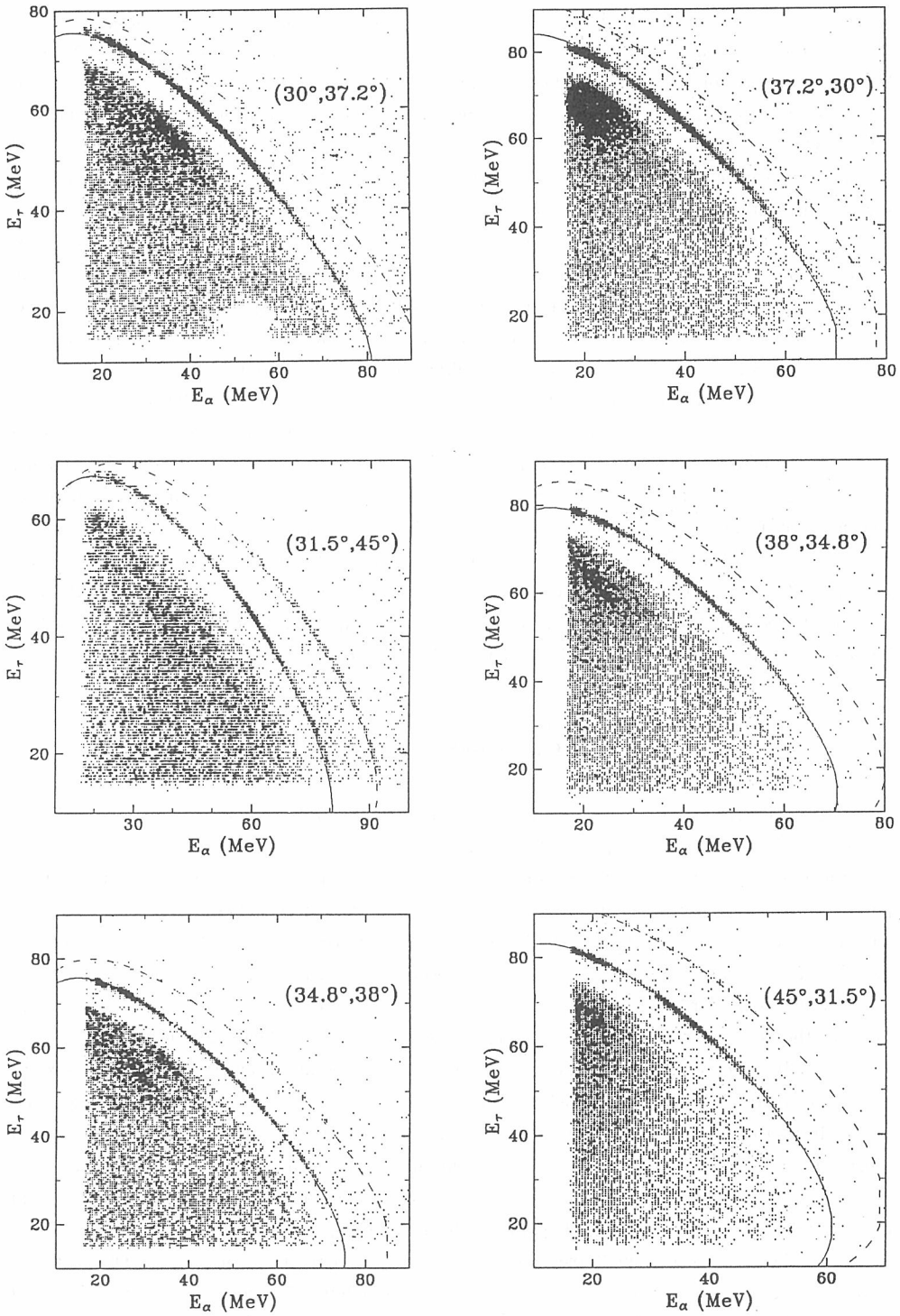

Fig. 1. The obtained two-dimensional energy spectra at all the angle pairs. Solid and dotted curves show the kinematical loci of ^{6}Li $(\alpha, \alpha\ \tau)^3$H and ^{6}Li $(\alpha, 2\alpha)^2$H three-body breakup reactions, respectively.

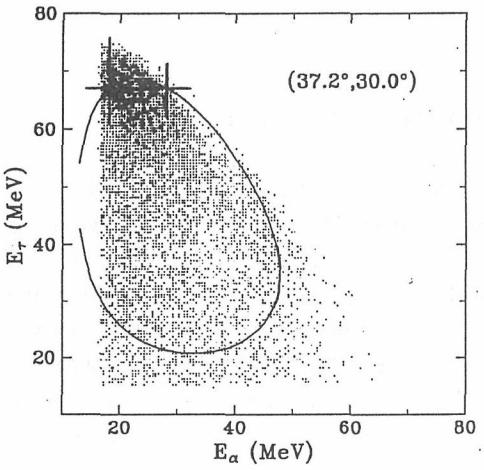

Fig. 2. The spectrum removed yields of the ^{6}Li (α, α ^{3}He)^{3}H three-body breakup reaction from the obtained two-dimensional energy spectrum at the angle pair of (37.2°, 30.0°). The solid curve presents the kinematical locus of the α*(α, α ^{3}He)n reaction, which corresponds to the elementary process of $\alpha + \alpha \rightarrow {}^{3}$He + ^{5}He in case of the spectator being rest. α* denotes an α cluster in ^{6}Li. Two crosses indicate the points where the α + n relative energy is 0.9 MeV, which corresponds to the energy of the g'nd state of ^{5}He.

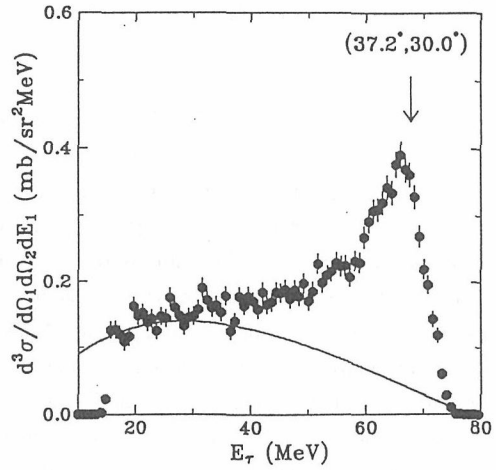

Fig. 3. The projected spectrum of fig. 2 on the E_τ axis, where an arrow shows the ^{3}He energy point where the spectator can be rest and the α-n relative energy can be 0.9 MeV. The solid curve presents the four-body phase space.

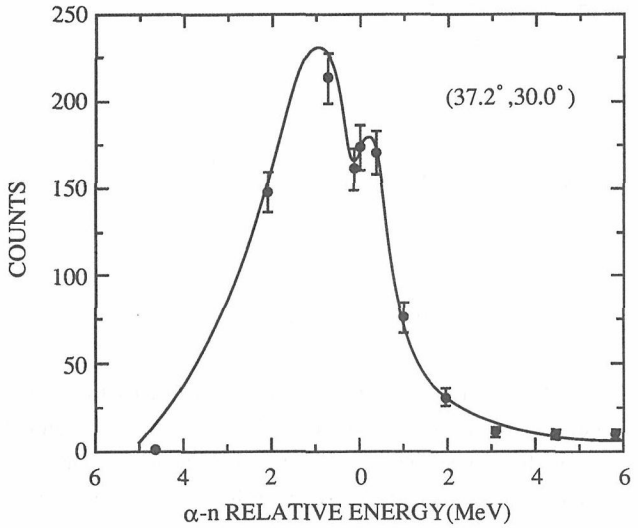

Fig. 4. Yields plotted on the locus in fig. 2 versus the α-n relative energy.

^{6}Li (α ,^{3}He^{5}He) ^{2}H reaction.

4. ESTIMATION OF DETECTION EFFICIENCY OF ^{5}He

An estimation of the detection efficiency of ^{5}He in our system was calculated based on the velocity vector diagram using the Monte Carlo method. The velocity vector diagram can show the region where α emitted from ^{5}He is kinematically allowed in the measured angle pairs. In this section, the drawing procedure of the velocity vector diagram, the calculation procedure and the estimation results are described in order. In order to draw the velocity vector diagram, velocities and emission angles of particles in both the initial and final states are required. First, non-relativistic kinematics of the ^{6}Li (α ,^{3}He^{5}He) ^{2}H reaction where a spectator d is rest is considered. In that case, since the spectator doesn't contribute to the reaction process, the three-body reaction is reduced to the two-body reaction

$$\alpha + \alpha^{*} \rightarrow {}^{3}\mathrm{He} + {}^{5}\mathrm{He}. \tag{1}$$

Now one simply expresses the reaction (1) as $a + b \rightarrow 1+2$. In general, the velocities of particles 1 and 2 are given by

$$V_1^{*} = \left\{ \frac{2m_2 \left(Q + \dfrac{m_a K_a}{m_a + m_b}\right)}{m_1 (m_1 + m_2)} \right\}^{\frac{1}{2}} \tag{2}$$

and

$$V_2^{*} = \left\{ \frac{2m_1 \left(Q + \dfrac{m_a K_a}{m_a + m_b}\right)}{m_2 (m_1 + m_2)} \right\}^{\frac{1}{2}}, \tag{3}$$

or

$$V_1 = V_g \cos\theta_1 \pm \left\{ (V_1^{*})^2 - (V_g \sin\theta_1)^2 \right\}^{\frac{1}{2}} \tag{4}$$

and

$$V_2 = \left\{ V_g^{\,2} + (V_2^{*})^2 - 2V_g V_2^{*} \cos\theta_1^{*} \right\}^{\frac{1}{2}}, \tag{5}$$

where m_i, θ_i, Q, K_a and V_g are the mass, the emission angle, of particle i, Q-value of the reaction (1), the kinetic energy of particle a in the laboratory system (LS) and the velocity of the center of mass, respectively. An asterisk in the formula denotes quantities in the center of mass system (CMS). Then θ_1^{*}, θ_2 and V_g are given by

$$\theta_1^{*} = \arccos \left\{ \frac{(V_1^{*})^2 + V_g^{\,2} - V_1^{\,2}}{2V_1^{*} V_g} \right\}, \tag{6}$$

$$\theta_2 = \arccos\left\{\frac{(V_2^*)^2 - V_2^2 - V_g^2}{2V_gV_2}\right\} \tag{7}$$

and

$$V_g = \frac{(2m_aK_a)^{\frac{1}{2}}}{m_a+m_b} . \tag{8}$$

Next, it is considered that ^{5}He decays into an α and a neutron with a relative energy ϵ. As before, denoting the decay process $^{5}\mathrm{He} \rightarrow \alpha + n$ as $2 \rightarrow 4+5$, the relation between the masses of particles 2, 4 and 5 can be written as

$$m_2 = m_4 + m_5 + \epsilon .$$

Furthermore, the velocity V_4^{R45} of particle 4 in the center of mass system of particles 4 and 5 (R45), is given by

$$V_4^{R45} = \left\{\frac{2\epsilon m_5}{m_4(m_4+m_5)}\right\}^{\frac{1}{2}} , \tag{9}$$

from the conservation laws of energy and momentum in R45. Finally, the velocity diagram of the reaction $a + b \rightarrow 1+2(4+5) \rightarrow 1+4+5$ can be drawn as fig. 5-a by using equations (2)-(9). As seen in this diagram, it is found the region kinematically allowed for the particle 4 is on the sphere whose radius and center are V_4^{R45} and the center of masses for particles 4 and 5, respectively.

As shown in fig. 5-a, one chooses the reaction point, the reaction plane and the direction of the beam as the origin O of xyz coordinate system, the xy plane and the y axis, respectively. Direction of the detector for α particle is defined by angles ζ and η. The detection region is restricted in the solid angle which is defined by the geometry of the slit system. As seen in the diagram, the detection efficiency is equal to the ratio of the penetrated area by the solid angle, (hatched area in the figure) to all the surface, on the sphere. The ratio can be calculated by using the Monte Carlo method. The coordinates of the center of the sphere, C are

$$\begin{pmatrix} x_C \\ y_C \\ z_C \end{pmatrix} = \begin{pmatrix} V_2\sin\theta_2 \\ V_2\cos\theta_2 \\ 0 \end{pmatrix} .$$

To simplify judgment whether a random event is in the area or not in the calculation, one rotates the diagram θ_2 on the z axis, $\zeta - \frac{\pi}{2}$ on the x axis and $\eta - \theta_2$ on the z axis so that the detector for α is the same direction as the y axis. Fig. 5-b shows the rotated diagram, in which the velocity vectors except V_2 and V_4^{R45} are not drawn. Then, the coordinates of C are given by

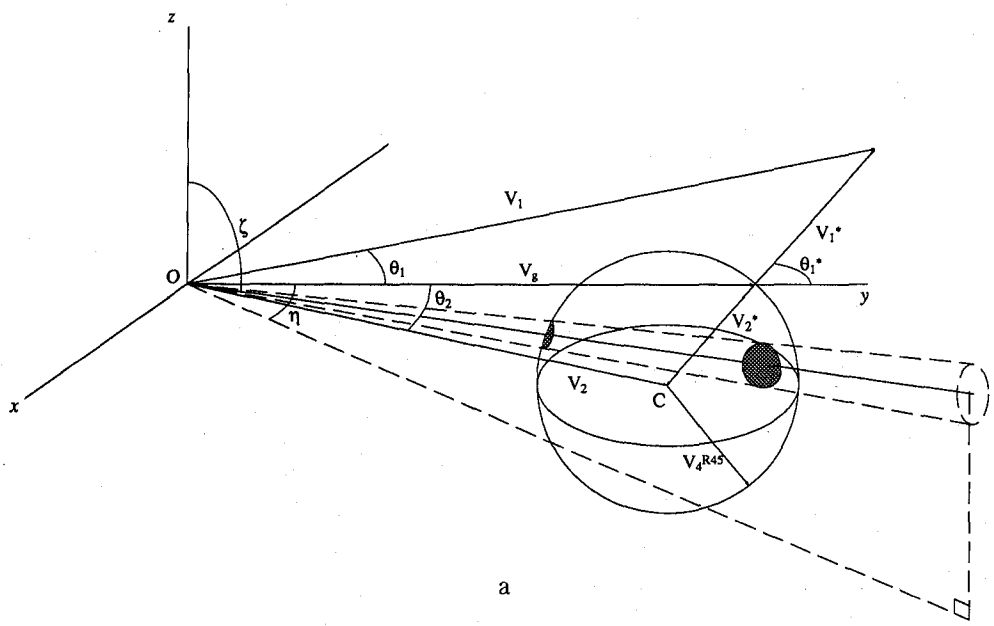

a

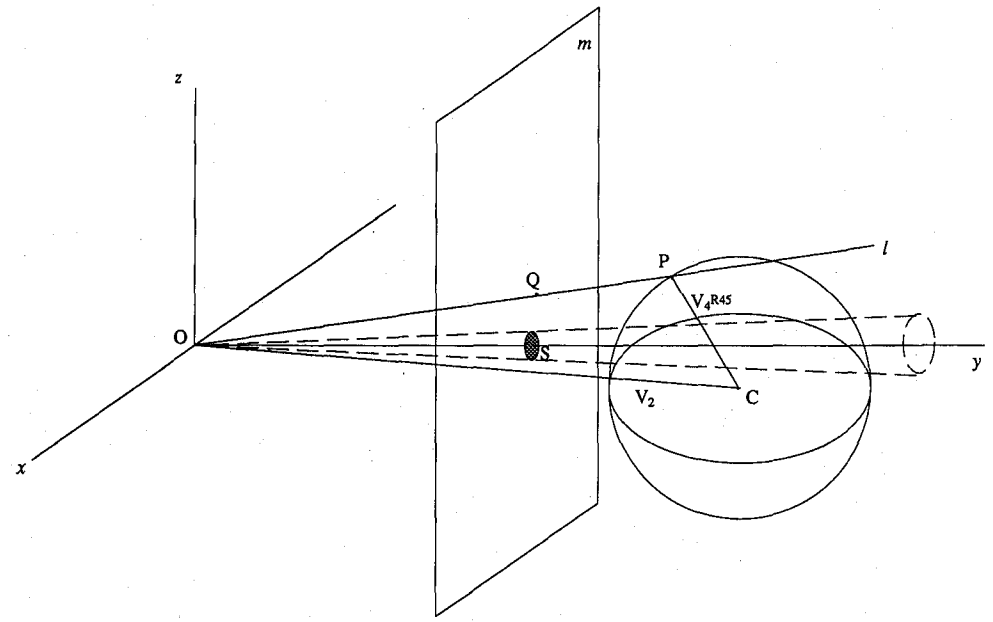

b

Fig. 5-a. The velocity vector diagram of the reaction $a + b \rightarrow 1+2(4+5) \rightarrow 1+4+5$.

Fig. 5-b. The rotated velocity vector diagram so that the detector for α is the same direction as the y axis, where the velocity vectors except V_2 and V_4^{R45} are not drawn.

$$\begin{pmatrix} x_C \\ y_C \\ z_C \end{pmatrix} = \begin{pmatrix} \cos(\zeta-\theta_2) & -\sin(\zeta-\theta_2) & 0 \\ \sin(\zeta-\theta_2) & \cos(\zeta-\theta_2) & 0 \\ 0 & 0 & 1 \end{pmatrix} \times \begin{pmatrix} 1 & 0 & 0 \\ 0 & \cos\eta & -\sin\eta \\ 0 & \sin\eta & \cos\eta \end{pmatrix} \times \begin{pmatrix} \cos\theta_2 & -\sin\theta_2 & 0 \\ \sin\theta_2 & \cos\theta_2 & 0 \\ 0 & 0 & 1 \end{pmatrix} \begin{pmatrix} V_2\sin\theta_2 \\ V_2\cos\theta_2 \\ 0 \end{pmatrix}.$$

In the fig. 5-b, P is a point on the sphere, l is the line through both O and P, L is the distance from the target center to the center of the slit, m is the plane parallel to the xz plane at $y = L$, Q is the cross point of l and m, and S is the cross section of the solid angle on the m. Giving P by a random event on the sphere, coordinates of P and Q are given by

$$\begin{pmatrix} x_P \\ y_P \\ z_P \end{pmatrix} = \begin{pmatrix} x_C \\ y_C \\ z_C \end{pmatrix} + V_4{}^{R45} \begin{pmatrix} \sin\{\arccos(1-2\text{rand})\}\cos(2\pi\,\text{rand}) \\ \sin\{\arccos(1-2\text{rand})\}\sin(2\pi\,\text{rand}) \\ 1\text{-}2\text{rand} \end{pmatrix}$$

and

$$\begin{pmatrix} x_Q \\ y_Q \\ z_Q \end{pmatrix} = \begin{pmatrix} Lx_P/y_P \\ L \\ Lz_P/y_P \end{pmatrix},$$

respectively, where "rand" is a function of generating random numbers from zero to one. If P is in this solid angle, Q must be involved in S. This boundary condition can be written by

$$f_S(x_Q, z_Q) \leq 0,$$

where f_S is a function expressing the boundary of S. The function in this experiment can be written as

$$f_S(x, z) = \begin{cases} z + \sqrt{4-x^2} + 2 & (z < -2) \\ |x| - 2 & (|z| \leq 2). \\ z - \sqrt{4-x^2} - 2 & (z > 2) \end{cases}$$

To estimate the ^{5}He detection efficiency in our slit system, the α-n relative energy ϵ was changed from 0 to 5 MeV by 0.2 MeV step and a million random events were generated for each values of ϵ. Moreover the calculated detection efficiency for each ϵ was weighted according to the spectrum of ^{5}He g'nd state predicted by the distorted wave Born approximation (DWBA), and summed for all ϵ. The obtained total detection efficiencies at each angle pair of (30.0°, 37.2°), (31.5°, 45.0°), (34.8°, 38.0°), (37.2°, 30.0°), (38.0°, 34.8°) and (45.0°, 31.5°) are about 4, 5, 4, 3, 4 and 0%, respectively.

5. ANALYSIS AND DISCUSSION

Four-body phase spaces for the ^{6}Li $(\alpha, \alpha\,^{3}\mathrm{He})$dn reaction were calculated for all angle pairs. Cross sections caused from only the four-body phase spaces were normalized to fit the lower energy part of the projected spectra. In fig. 3, the solid curve presents the four-body phase space, which was subtracted from the data as background yields. At zero recoil momentum of deuteron, the cross sections for the ^{6}Li $(\alpha, ^{3}\mathrm{He}^{5}\mathrm{He})$d reaction were deduced by considering the ^{5}He detection efficiencies. At the angle pair of (45.0°, 31.5°) data was excepted from this analysis, because the detection efficiency was very small. As a first step, the PWIA theory was used for the analysis. According to the PWIA theory, the cross sections for the elementary process can be written as follows.

$$\left(\frac{d\sigma}{d\Omega}\right)=\frac{d^{3}\sigma}{d\Omega_{1}d\Omega_{2}dE_{1}}/KF\cdot|\phi(K_{S})|^{2},$$

where $d^{3}\sigma/d\Omega_{1}d\Omega_{2}dE_{1}$, KF, $|\phi(K_{S})|$ and K_{s} are the projected three-body cross section for the ^{6}Li $(\alpha, ^{3}\mathrm{He}^{5}\mathrm{He})^{2}$H reaction, the kinematic factor, the momentum distribution of deuteron in ^{6}Li and the deuteron recoil momentum, respectively. The two body cross sections for the elementary process were deduced by using the measured three-body cross sections. Fig. 6 shows a comparison of the deduced cross sections and the free cross sections for the $^{4}\mathrm{He}(\alpha, ^{3}\mathrm{He})^{5}$He reaction at 120 MeV which were obtained in our recent experiment[11]. The deduced cross sections are normalized to the free cross section at $\theta_{c.m.}=60°$. The deduced cross

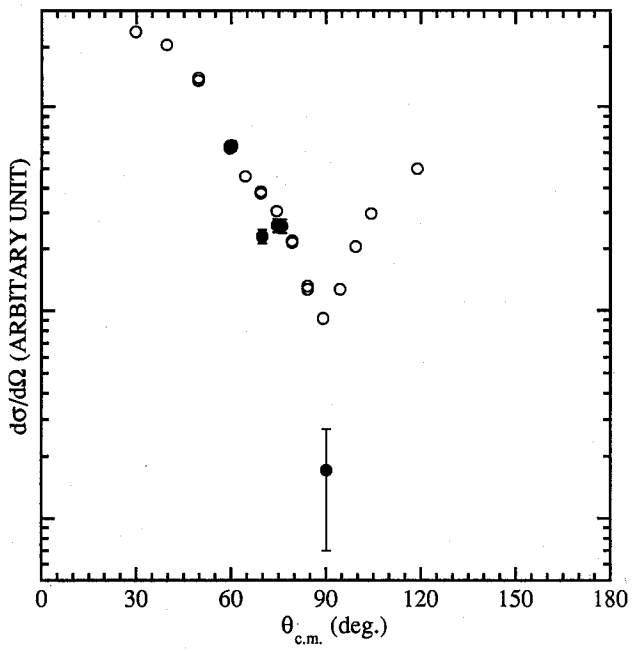

Fig. 6. The comparison of the deduced cross sections and the free cross sections for the ^{4}He $(\alpha, ^{3}\mathrm{He})^{5}$He reaction at 120 MeV. Closed circles show the deduced cross sections and open circles show the free cross sections.

sections seem to be almost agree with the angular distribution of the free cross sections. However an error of the deduced cross section at $\theta_{c.m.}$ =90° is very large and data points are less. Therefore, a measurement which covers wider range and has more accurate statistical precision will be desired. Also the angular distribution of the deduced cross sections for the (α,2α) QFS process are necessary to be compared with. Moreover, DWIA calculations with the distortion effects must be done. We plan to make these studies soon.

This experiment was performed at the RCNP under Program Numbers E29A09.

REFERENCES

(1) P. G. Roos, N. S. Chant, A. A. Cowley, D. A. Goldberg, H. D. Holmgren and R. Woody, III., *Phys. Rev.*, **C15**, 69 (1977).
(2) A. Nadasen, P. G. Roos, N. S. Chant, C. C. Chang, G. Ciangaru, H. F. Breuer, J. Wesick and E. Norbeck, *Phys. Rev.*, **C40**, 1289 (1989).
(3) C. W. Wang, N. S. Chant, P. G. Roos, A. Nadasen and T. A. Carey, *Phys. Rev.*, **C21**, 1705 (1980).
(4) A. Okihana, T. Konishi, R. E. Warner, D. Francis, M. Fujiwara, N. Matsuoka, K. Fukunaga, S. Kakigi, T. Hayashi, J. Kasagi, N. Koori, M. Tosaki and M. Greenfield, *Nucl. Phys.*, **A549**, 1 (1992).
(5) I. Slaus, R. G. Allas, L. A. Beach, R. O. Bondelid, E. L. Petersen, J. M. Lambert and D. L. Shannon, *Phys. Rev.*, **C8**, 444 (1973).
(6) R. G. Allas, L. A. Beach, R. O. Bondelid, E. M. Diener, E. L. Petersen, P. A. Treado, J. M. Lambert, R. A. Moyle, L. T. Myers, I. Slaus and P. Tomas, Few Body Problems in Nuclear and Particle Physics 422 (1975).
(7) J. Kasagi, T. Nakagawa, N. Sekine, T. Tōhei and H. Ueno, *Nucl. Phys.*, **A239**, 233 (1975).
(8) G. Calvi, M. Lattuada, D. Miljanić, F. Riggi, C. Spitaleri and M. Zadro, *Phys. Rev.*, **C41**, 1848 (1990).
(9) S. Blagus, C. Blyth, G. Calvi, O. Karban, M. Lattuada, D. Miljanić, F. Riggi, C. Spitaleri and M. Zadro, *Z. Phys.*, **A337**, 297 (1990).
(10) A. A. Cowley, P. G. Roos, N. S. Chant, R. Woody, III., H. D. Holmgren and D. A. Goldberg, *Phys. Rev.*, **C15**, 1650 (1977).
(11) R. E. Warner et al., to be published to *Phys. Rev.*, **C**